


Article

Spatial and Temporal Variations of Chlorophyll *a* and Primary Productivity in the Hangzhou Bay

Yiheng Wang^{1,2}, Jianfang Chen^{1,2,3,4}, Feng Zhou^{2,3,4,5} , Wei Zhang^{1,5} and Qiang Hao^{1,3,*}

- ¹ Key Laboratory of Marine Ecosystem Dynamics, Ministry of Natural Resources, Hangzhou 310012, China; wang0206@zju.edu.cn (Y.W.); jfchen@sio.org.cn (J.C.); zhangwei2020@sio.org.cn (W.Z.)
- ² Ocean College, Zhejiang University, Zhoushan 316021, China; zhoufeng@sio.org.cn
- ³ State Key Laboratory of Satellite Ocean Environment Dynamics, Second Institute of Oceanography, Ministry of Natural Resources, Hangzhou 310012, China
- ⁴ Observation and Research Station of Yangtze River Delta Marine Ecosystem, Ministry of Natural Resources, Zhoushan 316022, China
- ⁵ Zhejiang Key Laboratory of Nearshore Engineering Environment and Ecological Security, Hangzhou 310012, China
- * Correspondence: haoq@sio.org.cn; Tel.: +86-571-8196-3322

Abstract: The Hangzhou Bay (HZB) is an important part of the Zhoushan fishing ground, the most productive region in the Eastern China Seas. Although HZB remains eutrophication all year round, its chlorophyll *a* (Chl) and primary productivity (PP) are usually significantly lower than those in the adjacent waters. In the present study, we presented the Chl and PP distributions in the HZB and analyzed their correlations with environmental factors in four seasons. The field observation showed that Chl and PP had significant seasonal variations, and was highest in the summer ($1.66 \pm 0.61 \text{ mg} \cdot \text{m}^{-3}$ and $12.11 \pm 12.25 \text{ mg C} \cdot \text{m}^{-3} \cdot \text{h}^{-1}$, respectively). Total suspended matters (TSM) concentration was the key environmental factor that constrains PP in the study area. High concentration of TSM reduced light exposure (LE, the annual mean value was $0.92 \pm 0.81 \text{ Einstein} \cdot \text{m}^{-2} \cdot \text{day}^{-1}$) in the mixed layer of the HZB, which was much lower than the saturated light intensity of phytoplankton growth, and thus caused a strong light limitation in the HZB. However, the seasonal variations in the photosynthesis rates (P^B) and Chl did not coincide. This fact suggested that the growth rate was not the only factor controlling seasonal variations of phytoplankton biomass. In winter, the very high TSM and strong mixing might reduce the zooplankton grazing rate, and lead to a relatively high concentration of Chl during the very low LE and P^B period. These results implied that, in the HZB, the extremely turbid water could affect both phytoplankton growth and loss, which was probably the major mechanism responsible for the complex phytoplankton spatial and temporal variations.



Citation: Wang, Y.; Chen, J.; Zhou, F.; Zhang, W.; Hao, Q. Spatial and Temporal Variations of Chlorophyll *a* and Primary Productivity in the Hangzhou Bay. *J. Mar. Sci. Eng.* **2022**, *10*, 356. <https://doi.org/10.3390/jmse10030356>

Academic Editor: Sang Heon Lee

Received: 17 December 2021

Accepted: 5 February 2022

Published: 3 March 2022

Publisher's Note: MDPI stays neutral with regard to jurisdictional claims in published maps and institutional affiliations.



Copyright: © 2022 by the authors. Licensee MDPI, Basel, Switzerland. This article is an open access article distributed under the terms and conditions of the Creative Commons Attribution (CC BY) license (<https://creativecommons.org/licenses/by/4.0/>).

Keywords: Hangzhou Bay; chlorophyll *a*; primary productivity; light exposure; total suspended matters

1. Introduction

Primary productivity (PP) of phytoplankton is critical to marine fishery resources. In the coastal area of the East China Sea (ECS), terrigenous input, tidal mixing and coastal upwelling jointly control the material and energy required for phytoplankton growth and thus have important impacts on the distribution of coastal fisheries [1,2]. Affected by the Changjiang River and Zhejiang coastal upwelling, the largest fishing ground of the ECS appears around the Zhoushan Islands (29°30' S–31°00' S, 120°30' E–125°00' E), including the Zhoushan Islands, Hangzhou Bay (HZB) and the Changjiang Estuary (CJE) diluted water region, etc. [3–5]. The Zhoushan fishing ground is also the highest annual PP area in the ECS [3,4].

As an important part of the Zhoushan fishing ground, the HZB is the spawning and nursery ground of many economic species [6,7]. The HZB is one of the strongest tidal regions in the world [8] and is a highly eutrophic bay [9]. Influenced by its trumpet-like

shape and flat topography, tidal currents in the HZB are very strong and able to resuspend the bottom sediments. Hence, the total suspended matters (TSM) concentrations in the HZB are relatively high and can even reach $5000 \text{ mg}\cdot\text{dm}^{-3}$ [10,11]. In contrast, in its adjacent waters, such as the CJE and the Xiangshan Bay, the TSM concentrations are approximately $200 \text{ mg}\cdot\text{dm}^{-3}$ [12,13], two orders of magnitude lower than that in the HZB. These unique physical and chemical characteristics keep the chlorophyll *a* (Chl) and PP at a low level in the HZB.

Many studies have investigated the Chl dynamics in the HZB. Jia et al. reported the increasing severe eutrophication state of the entire HZB, but Chl concentrations ($0.54\text{--}3.42 \text{ mg}\cdot\text{m}^{-3}$) showed no significant change [14]. Liu et al. found that Chl concentrations changed significantly in the bay mouth of the HZB, with ranges of $0.20\text{--}6.96 \text{ mg}\cdot\text{m}^{-3}$ and $0.67\text{--}6.92 \text{ mg}\cdot\text{m}^{-3}$ in winter and summer, respectively [15]. Liu et al. also found that Chl concentrations in the HZB were generally less than $2 \text{ mg}\cdot\text{m}^{-3}$ in autumn and gradually increased from west to east [16]. Jiang et al. found that Chl concentrations in the HZB were lower in Spring ($<2 \text{ mg}\cdot\text{m}^{-3}$) but higher in summer ($>3 \text{ mg}\cdot\text{m}^{-3}$) with a high Chl concentration area at the northern side of the bay mouth [17]. Previous studies showed that the abundance of phytoplankton in the HZB was about one order of magnitude lower than its adjacent waters [18–20]. Despite being a part of the Zhoushan fishing ground, studies on PP in the HZB are scarce [15,16]. Due to the high concentration of TSM, the Secchi disk depth in the HZB was almost always less than 1 m [15]. Thus, PP in the HZB is very low with an average PP of less than $200 \text{ mg C}\cdot\text{m}^{-2}\cdot\text{day}^{-1}$ [11,15,16], while in the bay mouth of the HZB, PP can reach $320 \text{ mg C}\cdot\text{m}^{-2}\cdot\text{day}^{-1}$ during neap tides in summer [15]. Historical studies suggested that the light was the dominant factor limiting the growth of phytoplankton in the HZB [4,15,21]. However, little is known about the seasonal variations of Chl and PP in the HZB, and the in-situ observation and quantitative studies of related key environmental factor, such as light in the mixing layer, remain scarce.

In the present study, we aimed to reveal the spatial and temporal variations of phytoplankton and their environmental control in the HZB. Based on four seasons filed observations, we described the spatial and temporal variations of Chl and PP in the HZB and analyzed the related environmental factors, such as light exposure (LE) of phytoplankton in the mixed layer. We also compared the correlations of Chl, PP and photosynthesis rate with different environmental factors. Our work provides basic data on phytoplankton dynamics, and is helpful to understand environmental control of PP in the HZB.

2. Materials and Methods

2.1. Study Area

The HZB, adjacent to the CJE, is located in the east coast of China ($29^{\circ}50'\text{--}31^{\circ}00'$ N, $121^{\circ}00'\text{--}122^{\circ}00'$ E). The bay mouth of the HZB is adjacent to the CJE on the north, connected to the Zhoushan islands sea area on the east. The HZB is subjected to strong tides due to its trumpet-shaped characteristic and flat topography with an average water depth of less than 10 m [22]. Moreover, the HZB is significantly influenced by the Changjiang Diluted Water and a secondary plume of the Changjiang River entering the HZB on the north side [23].

Four field cruises in the HZB (i.e., July 2006 (summer); December 2006 (winter); April 2007 (spring); October 2007 (autumn)) were conducted (Figure 1). In total, 83 stations (21 stations in July 2006, 21 stations in December 2006, 20 stations in April 2007 and 21 stations in October 2007, respectively) were set up for Chl and environmental parameters. We fully considered the variation in environmental gradient for PP stations to ensure that PP stations contained different salinity and bottom depth. Thus, 18 PP stations (5 stations in July 2006, 6 stations in December 2006, 4 stations in April 2007 and 3 stations in October 2007, respectively) were set up (Figure 1).

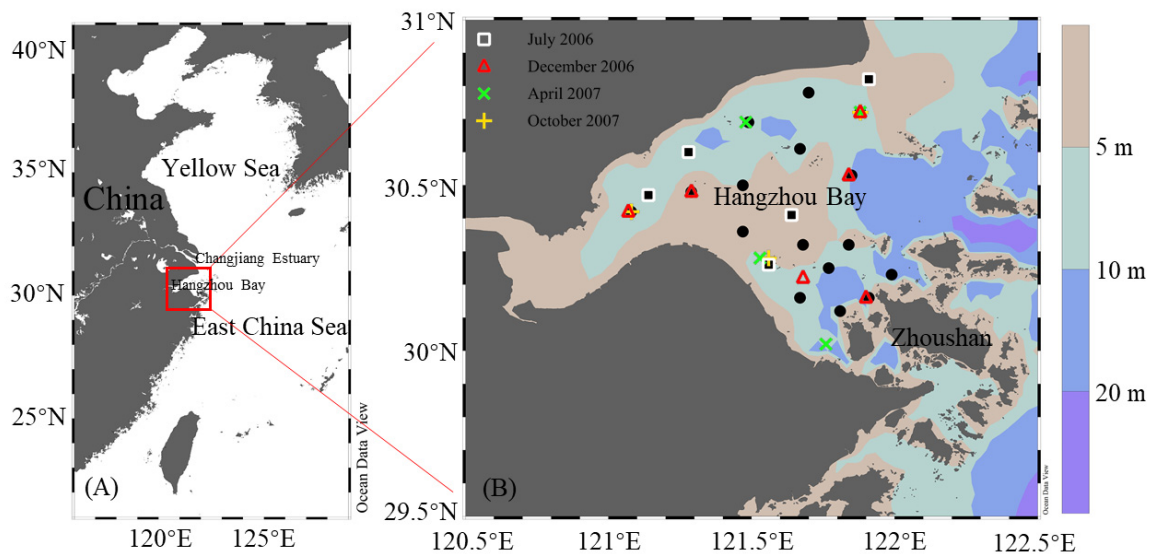


Figure 1. Area bounded by the red box in (A) shows the studied location in and off the HZB. (B) shows the sampling stations and the water depth in the HZB, black dots are Chl and environmental stations, and PP stations in July 2006, December 2006, April 2007 and October 2007 are shaped as white square, red triangles, green X and yellow +, respectively.

2.2. Environmental Parameters

A Rosette sampler was used to collect seawater samples at the surface and bottom layers of the HZB. 100 mL of seawater filtered by 0.45 μm acetate membrane was collected and fixed with 0.3 mL of 35 $\text{g}\cdot\text{dm}^{-3}$ HgCl_2 for storage. Dissolved inorganic nitrogen (DIN, $\text{NO}_x + \text{NH}_4^+$), dissolved inorganic phosphorus (DIP) and dissolved silicate (DSi) were measured by Skalar San++ according to the National Standard of the People’s Republic of China (GB12763.4-91).

TSM was measured using the weighing method. The surface and bottom layer seawater samples were filtered by Whatman GF/F filter membrane (prepared at 450 $^\circ\text{C}$ for 2 h and weighed before). The membrane was cryopreserved and brought back to the laboratory. In the laboratory, the thawed membrane was placed in the muffle furnace at 500 $^\circ\text{C}$ for 2 h, equilibrated with a silica gel dryer and weighed until the weight no longer changed. Finally, the TSM was calculated using the result of weighing and the volume of the sample.

LE can be calculated from the sea surface light intensity (i.e., photosynthetically available radiation (PAR), obtained from NASA’s sea surface light intensity data product (<https://oceancolor.gsfc.nasa.gov>, accessed on 2 April 2021) [24]), and the formula is as follow [3]:

$$LE = \frac{I_0}{\text{MLD}\cdot K} \cdot (1 - e^{-\text{MLD}\cdot K})$$

where I_0 is the sea surface light intensity ($\text{Einstein}\cdot\text{m}^{-2}\cdot\text{day}^{-1}$), MLD is the mixed layer depth (m), K is the light attenuation. MLD is related to water stability and K is controlled by TSM. In this study, MLD is the first depth where $\Delta\text{Temperature} > 0.5\text{ }^\circ\text{C}\cdot\text{m}^{-1}$, K is calculated from Secchi disk depth according to the method proposed by Castillo-Ramirez et al. [25].

2.3. Chlorophyll a

Chl concentrations ($\text{mg}\cdot\text{m}^{-3}$) were determined by fluorimetry after 50 mL surface and bottom layer seawater samples were collected, respectively. The seawater samples were filtered by 200 μm bolting-silk to remove zooplankton, and then filtered by Whatman GF/F filter membrane. The Whatman GF/F filter membrane containing phytoplankton was extracted with 90% acetone for 18 h in darkness and at $-20\text{ }^\circ\text{C}$. Then, the Turner Designs 10 AU Fluorometer was used to determine the concentration in the extraction fluid. The determination and calculation were performed by following the method in [26].

2.4. Primary Productivity and Photosynthetic Rate

PP and photosynthetic rate (P^B) were determined using the ^{14}C isotope tracer method developed by Nielsen and modified by Ning et al. and Evans et al. [27–29]. The surface seawater samples were filtered with 200 μm bolting-silk to remove zooplankton. Then, they were injected into two white culture bottles and one black culture bottle. A certain amount of $NaH^{14}CO_3$ tracer was added into each culture bottle successively, and placed on the deck to simulate field culture at surface temperature. Different neutral light fading materials were selected to control the light intensity of the simulated incubator. Meanwhile, surface seawater was cyclically pumped to control the temperature. The incubator was cultured for 6 h. After culture, the phytoplankton samples were collected using Whatman GF/F filter membrane. The membrane was fumigated with concentrated hydrochloric acid, and then placed in scintillation bottles for drying and preservation at low temperature. The samples were taken back to the laboratory for determination on a PE 2900 liquid scintillation counter. PP was calculated according to the formula recommended by Parsons [30], and P^B was calculated as the ratio of surface PP to Chl.

2.5. Data Analysis

Considering the strong mixing in the HZB, in this study, the mean Chl concentrations and chemical variables in the mixed layer were used in the analysis. The distribution of each parameter was drawn using Ocean Data View 5.5.1 [31]. R language was used for data analysis, and Pearson was used to test the correlation between Chl, PP and environmental factors.

3. Results

3.1. Environmental Parameters

In the HZB, the surface temperature and salinity varied greatly in different seasons, and their distributions are shown in Appendix A (Figure A1). The surface temperature was higher in summer (27.87 ± 1.08 °C) and autumn (19.83 ± 0.62 °C), and lower in spring (14.93 ± 0.63 °C) and winter (7.83 ± 1.05 °C); while the mean surface salinity was higher in winter (19.50 ± 3.09) and spring (19.06 ± 6.31), and lower in summer (13.90 ± 8.19) and autumn (13.58 ± 3.84) (Table 1). In addition, there was a significant intrusion of high salinity seawater in the bay mouth in summer (Figure A1).

Table 1. Chl, PP, P^B and environmental parameters recorded in the HZB in each cruise (mean \pm SD).

Parameters	July 2006	December 2006	April 2007	October 2007
Chl ($mg \cdot m^{-3}$)	1.66 \pm 0.61	1.50 \pm 0.51	1.00 \pm 0.31	0.90 \pm 0.41
PP ($mg \ C \cdot m^{-3} \cdot h^{-1}$)	12.11 \pm 12.25	1.32 \pm 1.02	2.10 \pm 1.18	0.20 \pm 0.12
P^B ($mg \ C \cdot (mg \ Chl \cdot h)^{-1}$)	5.46 \pm 3.64	0.88 \pm 0.30	2.33 \pm 1.45	0.20 \pm 0.01
Surface Temperature (°C)	27.87 \pm 1.08	7.83 \pm 1.05	14.93 \pm 0.63	19.83 \pm 0.62
Surface Salinity	13.90 \pm 8.19	19.50 \pm 3.09	19.06 \pm 6.31	13.58 \pm 3.84
MLD (m)	8 \pm 2	9 \pm 2	9 \pm 2	11 \pm 3
PAR ($Einstein \cdot m^{-2} \cdot day^{-1}$)	34.31 \pm 3.50	18.99 \pm 7.80	33.50 \pm 4.19	22.17 \pm 1.47
LE ($Einstein \cdot m^{-2} \cdot day^{-1}$)	1.89 \pm 0.98	0.43 \pm 0.19	0.87 \pm 0.35	0.46 \pm 0.13
DIN ($\mu mol \cdot dm^{-3}$)	89.81 \pm 31.62	93.75 \pm 28.37	99.15 \pm 39.07	74.33 \pm 22.40
DIP ($\mu mol \cdot dm^{-3}$)	1.45 \pm 0.32	1.44 \pm 0.19	1.18 \pm 0.11	1.61 \pm 0.18
DSi ($\mu mol \cdot dm^{-3}$)	62.96 \pm 21.30	63.99 \pm 11.03	53.07 \pm 11.20	83.39 \pm 12.77
N/P (dimensionless)	60.80 \pm 10.51	64.43 \pm 13.42	82.67 \pm 27.27	45.92 \pm 11.56
N/Si (dimensionless)	1.43 \pm 0.15	1.44 \pm 0.19	1.80 \pm 0.34	0.87 \pm 0.13
Si/P (dimensionless)	42.77 \pm 7.82	44.52 \pm 4.51	44.81 \pm 6.63	51.98 \pm 5.97
TSM ($g \cdot dm^{-3}$)	0.56 \pm 0.35	2.34 \pm 1.67	3.01 \pm 2.04	2.41 \pm 1.63

Note: Chl, LE, DIN, DIP, DSi, N/P, N/Si, Si/P and TSM were the mean values in the mixed layer, PP, P^B , Temperature, Salinity and PAR were the surface values.

The nutrient concentrations in the HZB were relatively high and had significant spatial distributions (Figure 2). DIN, DIP and DSi showed decreasing trends from west to east in each season (Figure 2A–L). N/P, N/Si and Si/P also demonstrated declining trends from west to east in each season (Figure 2M–X).

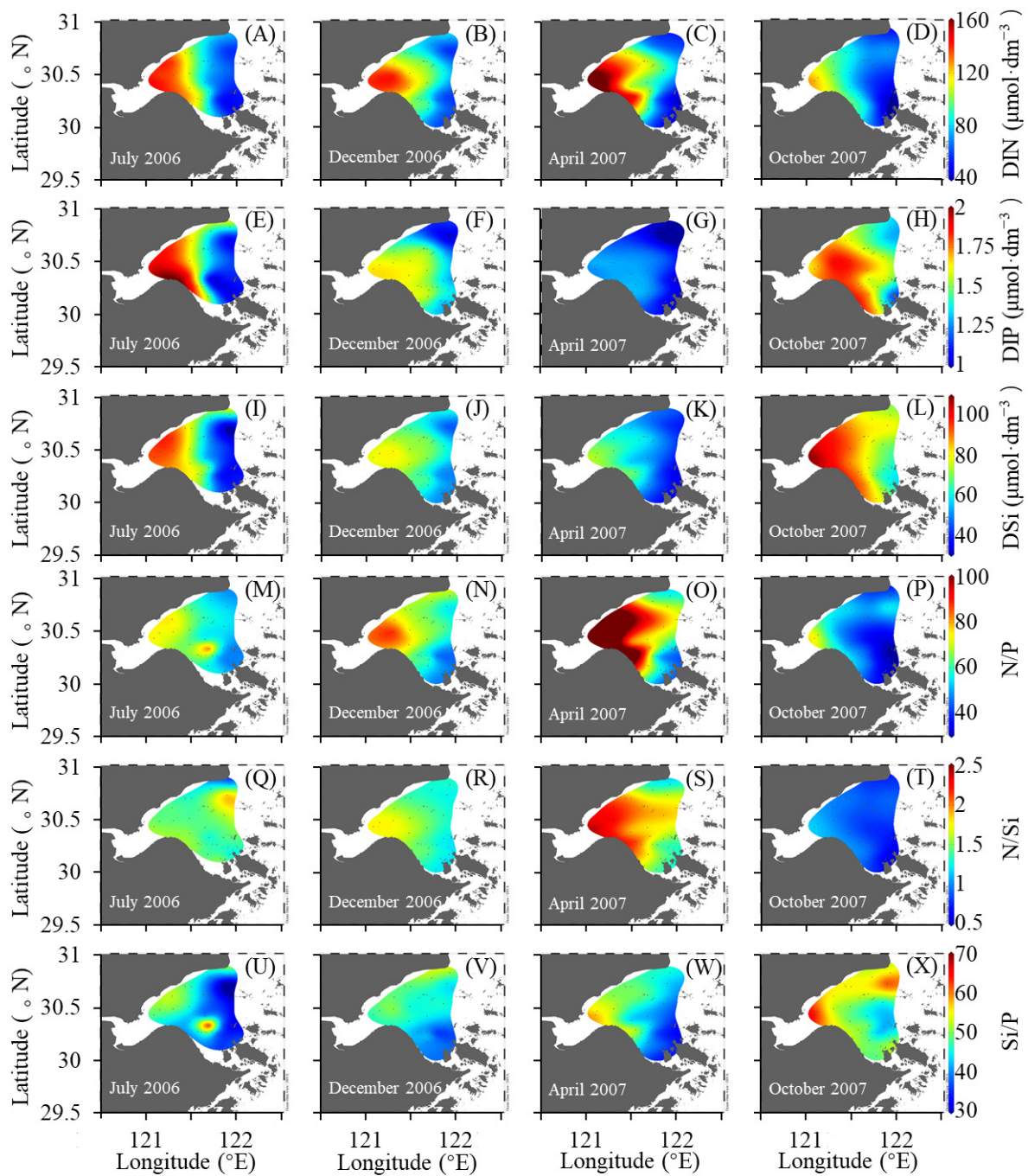


Figure 2. Spatial and temporal variations of (A–D) DIN ($\mu\text{mol}\cdot\text{dm}^{-3}$), (E–H) DIP ($\mu\text{mol}\cdot\text{dm}^{-3}$), (I–L) DSi ($\mu\text{mol}\cdot\text{dm}^{-3}$), (M–P) N/P, (Q–T) N/Si and (U–X) Si/P.

As shown in Figure 3, the TSM in the HZB had significant seasonal variation. TSM in summer ($0.56\text{ g}\cdot\text{dm}^{-3}$) was much lower than in other seasons (mean TSM in winter, spring and autumn were $2.34\text{ g}\cdot\text{dm}^{-3}$, $3.01\text{ g}\cdot\text{dm}^{-3}$, and $2.41\text{ g}\cdot\text{dm}^{-3}$, respectively), about a quarter to a fifth of them (Table 1). Although PAR in the HZB was not low, influenced by high TSM concentrations, LE was usually only 1–5% of PAR. The seasonal variation of LE was ranked in the order summer > spring > autumn > winter (Figure A2), not wholly consistent with TSM. The mean PAR in summer ($34.31 \pm 3.50\text{ Einstein}\cdot\text{m}^{-2}\cdot\text{day}^{-1}$) and spring ($33.50 \pm 4.19\text{ Einstein}\cdot\text{m}^{-2}\cdot\text{day}^{-1}$) was similar, but the mean LE in summer ($1.89 \pm 0.98\text{ Einstein}\cdot\text{m}^{-2}\cdot\text{day}^{-1}$) was about twice as high as that in spring ($0.87 \pm 0.35\text{ Einstein}\cdot\text{m}^{-2}\cdot\text{day}^{-1}$) (Table 1). In addition, there was no significant difference

between mean LE in autumn ($0.46 \pm 0.13 \text{ Einstein}\cdot\text{m}^{-2}\cdot\text{day}^{-1}$) and winter ($0.43 \pm 0.19 \text{ Einstein}\cdot\text{m}^{-2}\cdot\text{day}^{-1}$) (Table 1). The highest LE ($4.29 \text{ Einstein}\cdot\text{m}^{-2}\cdot\text{day}^{-1}$) occurred in the middle of the bay mouth in summer (Figure 3I), consistent with the lowest TSM (Figure 3A).

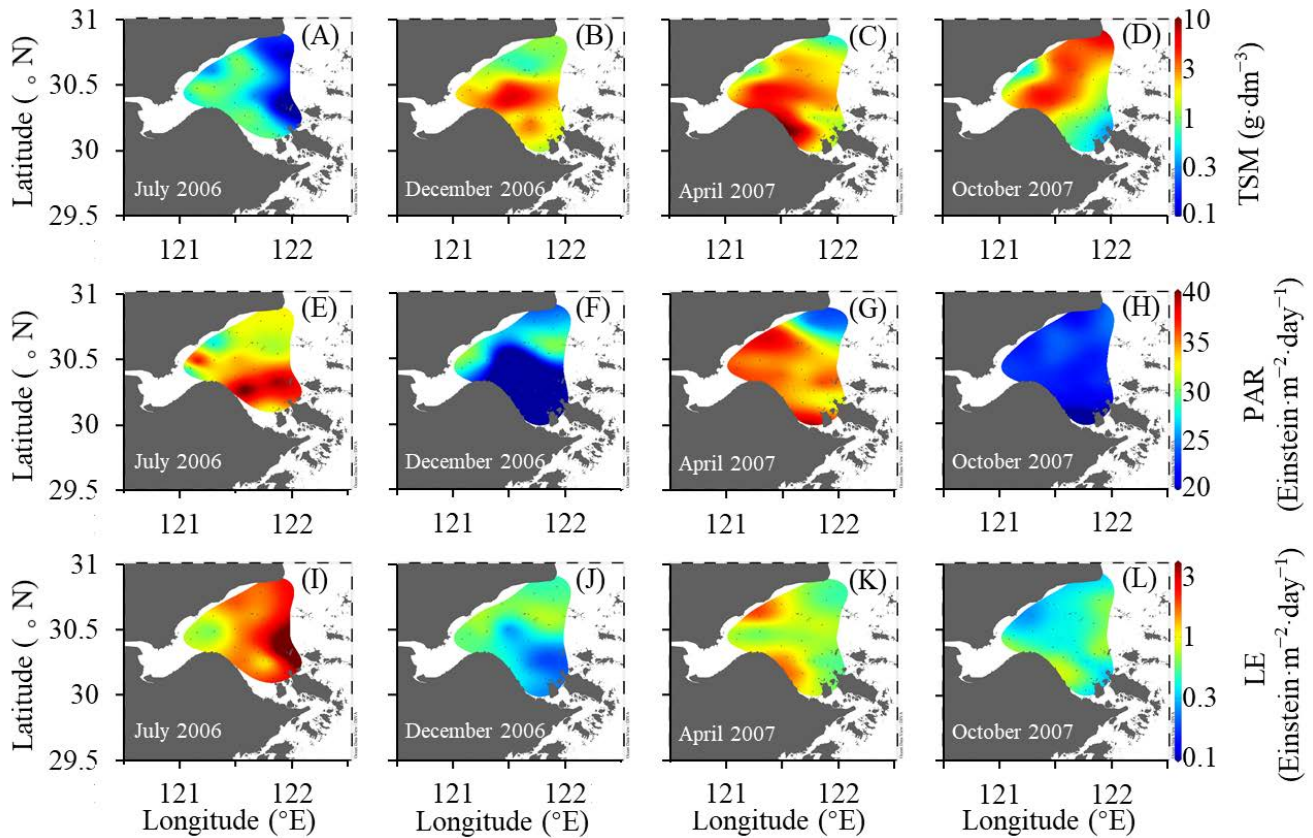


Figure 3. Spatial and temporal variations of (A–D) TSM ($\text{g}\cdot\text{dm}^{-3}$), (E–H) PAR ($\text{Einstein}\cdot\text{m}^{-2}\cdot\text{day}^{-1}$) and (I–L) LE ($\text{Einstein}\cdot\text{m}^{-2}\cdot\text{day}^{-1}$).

3.2. Distribution of Chl

As shown in Figure 4, Chl in the HZB had significant seasonal variations. Chl concentrations were higher in summer ($1.66 \pm 0.61 \text{ mg}\cdot\text{m}^{-3}$) and winter ($1.50 \pm 0.51 \text{ mg}\cdot\text{m}^{-3}$), and lower in spring ($1.00 \pm 0.31 \text{ mg}\cdot\text{m}^{-3}$) and autumn ($0.90 \pm 0.41 \text{ mg}\cdot\text{m}^{-3}$). In addition, high Chl concentrations ($>2 \text{ mg}\cdot\text{m}^{-3}$) only occurred in summer and winter, but there are no found in spring and autumn (Figure 4).

In summer, the range of Chl concentrations was $0.84\text{--}2.97 \text{ mg}\cdot\text{m}^{-3}$. High Chl ($>2 \text{ mg}\cdot\text{m}^{-3}$) in summer occurred in the east of the HZB (Figure 4), and the lowest Chl concentration ($0.84 \text{ mg}\cdot\text{m}^{-3}$) occurred in the south side of the HZB (Figure 4A). The distribution of Chl in summer was contrary to that of TSM, and both exhibited significant variation trends from west to east. In winter, the range of Chl concentrations was $0.91\text{--}2.34 \text{ mg}\cdot\text{m}^{-3}$. And high Chl ($>2 \text{ mg}\cdot\text{m}^{-3}$) in winter occurred in the middle of the HZB, the northwest side and north of the bay mouth (Figure 4B). In spring, the range of Chl concentrations was $0.45\text{--}1.62 \text{ mg}\cdot\text{m}^{-3}$. The highest and lowest Chl in spring occurred in the south and north of the study area (Figure 4C), respectively, opposite to TSM. In autumn, the range of Chl concentrations was $0.28\text{--}1.69 \text{ mg}\cdot\text{m}^{-3}$. Chl in autumn was higher in the east and west and lower in the north and south (Figure 4D).

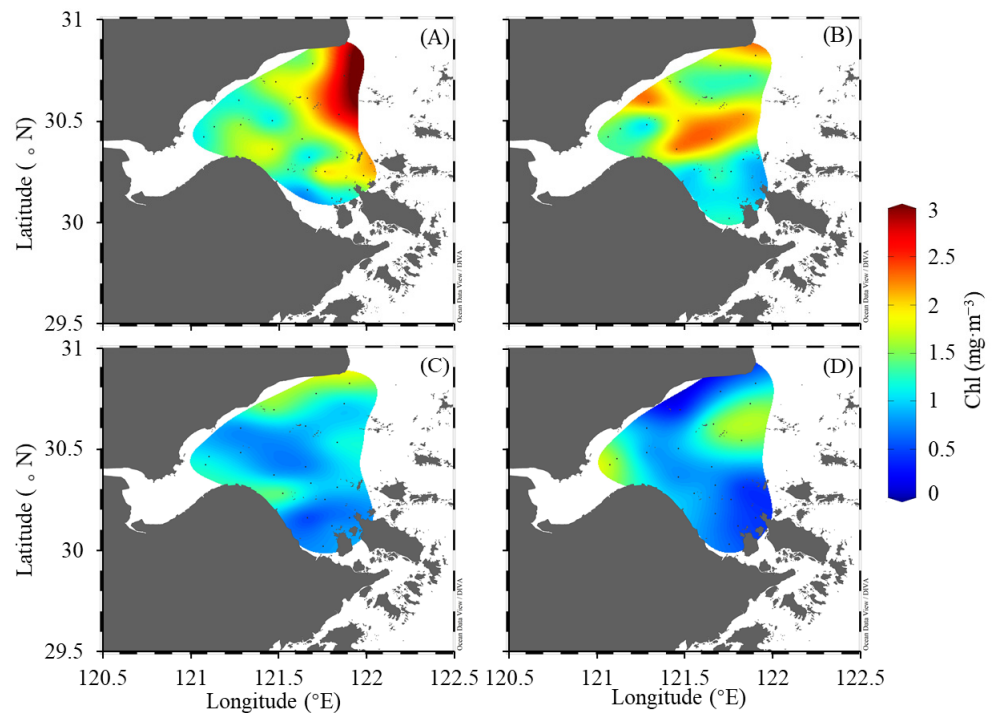


Figure 4. Spatial and temporal variations of Chl ($\text{mg}\cdot\text{m}^{-3}$) in (A) July 2006, (B) December 2006, (C) April 2007 and (D) autumn.

3.3. Surface PP and P^B

PP in the HZB ranged from $0.11\text{--}30.38 \text{ mg C}\cdot\text{m}^{-3}\cdot\text{h}^{-1}$ and had a significant variation of summer > spring > winter > autumn (Figure A2). The highest PP in summer ($30.38 \text{ mg C}\cdot\text{m}^{-3}\cdot\text{h}^{-1}$) occurred in the north side of the bay mouth (Figure 5A). PP in summer experienced a decreasing trend from east to west (Figure 5A). The mean PP in winter was $1.32 \pm 1.02 \text{ mg C}\cdot\text{m}^{-3}\cdot\text{h}^{-1}$, and its distribution trend was similar to that of Chl, where both high-value areas occurred in the middle of the bay mouth (Figure 5B). Although Chl in spring was lower than in winter, the mean PP in spring ($2.10 \pm 1.18 \text{ mg C}\cdot\text{m}^{-3}\cdot\text{h}^{-1}$) was higher than in winter. High PP in spring occurred in the north of the HZB with a downward trend from north to south (Figure 5C). The mean PP in autumn was only $0.20 \pm 0.12 \text{ mg C}\cdot\text{m}^{-3}\cdot\text{h}^{-1}$, almost one order of magnitude lower than those in other seasons, indicating that autumn was a typical period of low productivity.

Our results showed that PP had the similar spatial distribution as PP in each season (Figure 6). P^B also had significant seasonal variations (Figure A2). In this study, P^B in the HZB ranged from $0.19\text{--}10.32 \text{ mg C}\cdot(\text{mg Chl}\cdot\text{h})^{-1}$, with the annual mean value of $2.36 \pm 2.82 \text{ mg C}\cdot(\text{mg Chl}\cdot\text{h})^{-1}$. P^B was higher in summer ($5.46 \pm 3.64 \text{ mg C}\cdot(\text{mg Chl}\cdot\text{h})^{-1}$) and spring ($2.33 \pm 1.45 \text{ mg C}\cdot(\text{mg Chl}\cdot\text{h})^{-1}$), while lower in winter ($0.88 \pm 0.30 \text{ mg C}\cdot(\text{mg Chl}\cdot\text{h})^{-1}$) and autumn ($0.20 \pm 0.01 \text{ mg C}\cdot(\text{mg Chl}\cdot\text{h})^{-1}$) (Table 1).

3.4. Correlations among Biological and Environment Parameters

We compared Pearson correlation among biological and environmental parameters in the different seasons. As shown in Figure 7, nutrients usually had significant negative correlations with salinity (Figure 7) in the four seasons, inferring nutrients' variations dominated by eutrophic terrestrial input in the HZB. However, biological parameters, such as Chl, PP and P^B , had no relationship with nutrients. It suggested that nutrient variations neither affected phytoplankton biomass nor its growth. Although high TSM is the major reason for low LE in the HZB, the LE also had significant correlations between PAR or MLD in different seasons. This meant that LE variability in each season was complex, and LE distributions also could be partly affected by PAR and MLD. Note that correlations

among biological and environmental parameters were not consistent in different seasons. It meant that, in a year, phytoplankton variations could not be explained by using a single environment parameter.

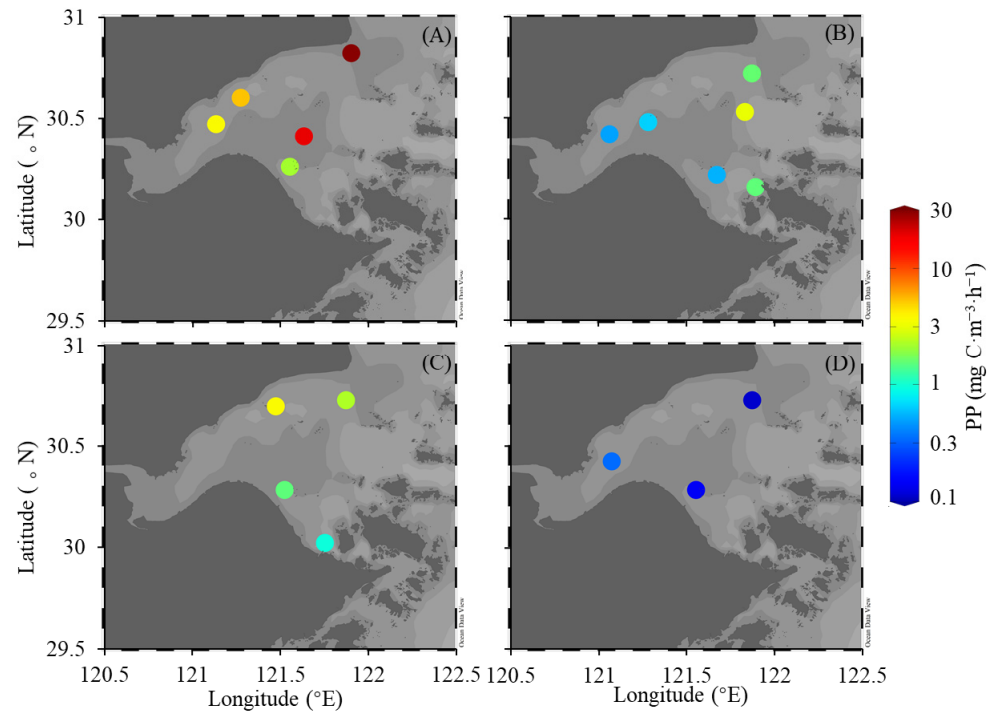


Figure 5. Spatial and temporal variations of PP ($\text{mg C}\cdot\text{m}^{-3}\cdot\text{h}^{-1}$) in (A) July 2006, (B) December 2006, (C) April 2007 and (D) October 2007.

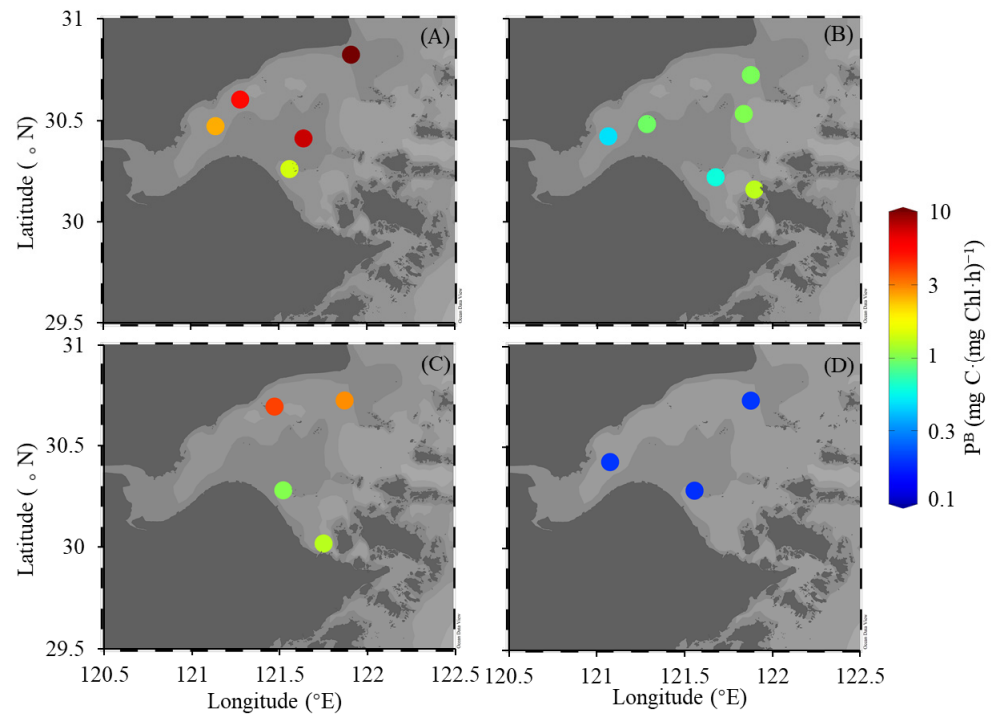


Figure 6. Spatial and temporal variations P^B ($\text{mg C}\cdot(\text{mg Chl}\cdot\text{h})^{-1}$) in (A) July 2006, (B) December 2006, (C) April 2007 and (D) October 2007.

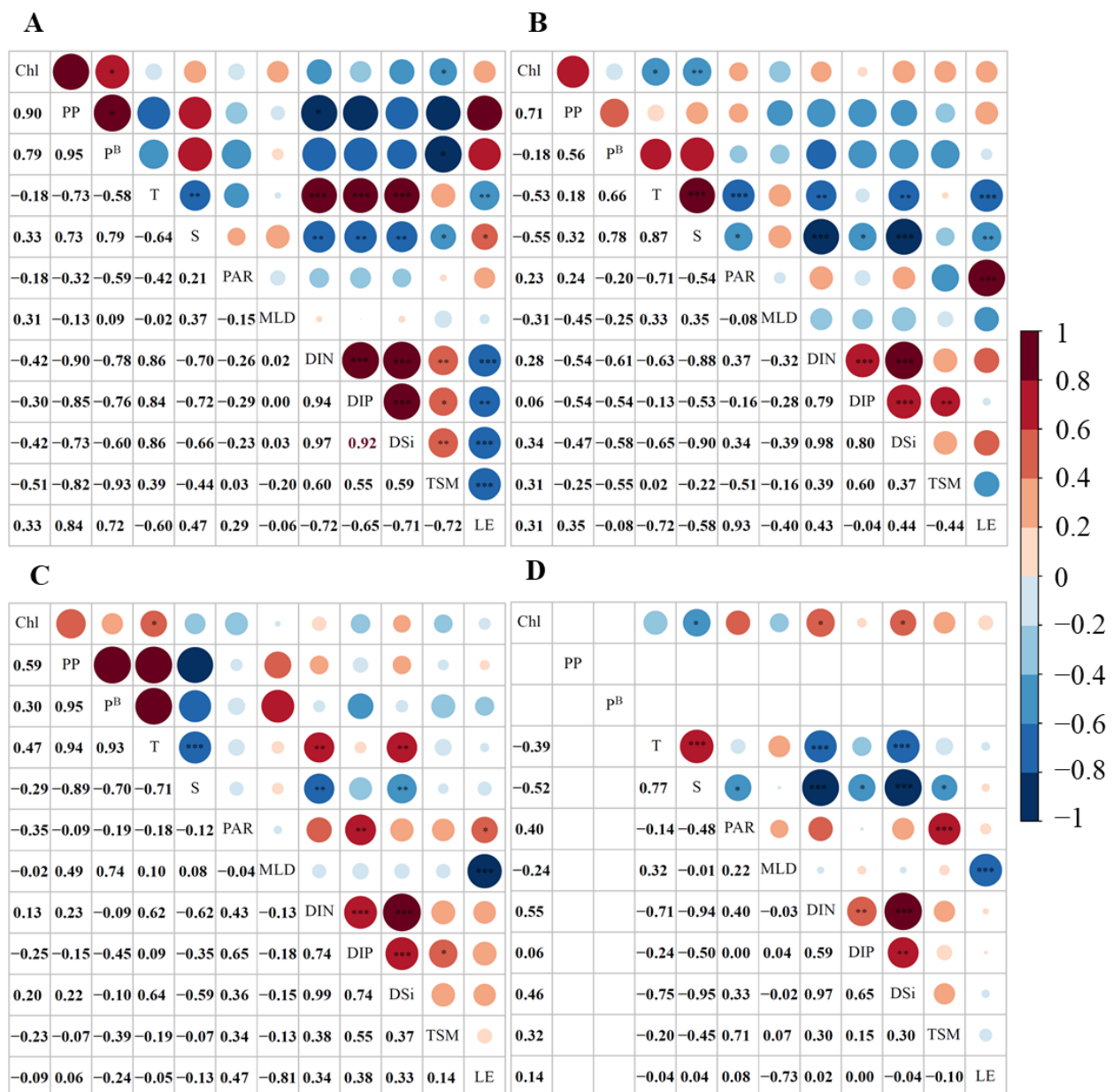


Figure 7. Pearson correlation analysis matrix among biological and environmental parameters in (A) July 2006, (B) December 2006, (C) April 2007 and (D) October 2007, where T is surface temperature ($^{\circ}\text{C}$), and S is surface salinity. *: $p < 0.05$; **: $p < 0.01$; ***: $p < 0.001$. In October 2007, the correlations between PP, P^B and other parameters are not available because of the small amount of data.

4. Discussion

4.1. Dynamics of Chl

Historical studies showed that the variation of Chl in the HZB was usually ranged within one order of magnitude, and the high Chl usually occurs in summer [14,15,17]. Long-term observations of Jia et al. showed that the Chl concentrations varied from 0.54 to 3.42 $\text{mg}\cdot\text{m}^{-3}$ during 1992–2012 [14], and Chl concentrations were higher in summer but lower in spring [17]. Our results showed that the Chl level and seasonal variation were consistent with those in previous studies. Our study found that Chl had significant spatial and temporal variations in the HZB, ranging from 0.45 to 2.97 $\text{mg}\cdot\text{m}^{-3}$. The annual highest Chl (2.97 $\text{mg}\cdot\text{m}^{-3}$) occurred in the northern side of the bay mouth in summer (Figure 4A), and the annual lowest Chl (0.28 $\text{mg}\cdot\text{m}^{-3}$) occurred in the northern side of the bay mouth in

autumn (Figure 4D). The Chl in HZB increased with the water depth in summer, and the high Chl occurred in the area near the CJE, consistent with the historical data [17]. However, in other seasons, the spatial distribution of Chl in HZB seemed to have no clear rules.

Our results showed that the annual mean concentrations of DIN, DIP and DSi in the HZB were $89.14 \mu\text{mol}\cdot\text{dm}^{-3}$, $1.42 \mu\text{mol}\cdot\text{dm}^{-3}$ and $65.85 \mu\text{mol}\cdot\text{dm}^{-3}$ (Table 1), respectively, much higher than the limitation thresholds (DIN = $1 \mu\text{mol}\cdot\text{dm}^{-3}$, DIP = $0.1 \mu\text{mol}\cdot\text{dm}^{-3}$ and DSi = $2 \mu\text{mol}\cdot\text{dm}^{-3}$, suggested by Justić et al [32]). The mean values of N/P and Si/P were higher four and three times than Redfield ratio [33], respectively. Notably, although N/P and Si/P indicated that DIP would deplete first, the DIP concentration is still higher than the limitation threshold [34]. This suggested that the HZB was a potential phosphorus limited region [35]. However, there was no significant correlation between Chl and nutrients in the HZB (Figure 7). This suggested that nutrients were not the control factor for phytoplankton, which was consistent with the previous study [14].

Some literature suggested that water temperature was an important factor affecting the ECS nearshore phytoplankton [36,37]. However, our results showed (Figure 7) that Chl and temperature changes in HZB lacked consistency, and the correlation coefficient between the two was not high ($r^2 < 0.3$). This suggests that temperature is not an important factor affecting phytoplankton changes and that its effect on phytoplankton may be indirect [3].

We compared the Chl levels in different highly turbid estuaries (Table 2) and found that the Chl in the HZB varied within a smaller range than other estuaries. In addition, the Chl level in the HZB was lower than in other estuaries. For example, the CJE is adjacent to the HZB with similar nutrient levels, but the Chl in the CJE is much higher than the HZB. The reason could be that the very low LE inhibited the phytoplankton blooming, and there was no bloom season because of the all-year-round strong light limitation in the HZB. The annual mean LE in the HZB was merely $0.92 \pm 0.81 \text{ Einstein}\cdot\text{m}^{-2}\cdot\text{day}^{-1}$, which was about only 10% of the mean LE in the coastal waters of China [3]. Hao et al. suggested that, due to the seasonal increase of TSM and MLD, light limitation usually occurred in the winter half-year in the offshore waters of the ECS [3]. However, in the HZB, the light limitation existed in any season because of the extremely high TSM induced by tide mixing. In other sea areas, the light limitation tends to be intermittent, resulting in localized or seasonal blooms, and thus the Chl in these areas usually change greatly.

Table 2. Main characteristics (abiotic environment and Chl) of some turbid estuaries including the HZB.

Study Area	Charente	Plata River	Changjiang	Yellow River	Hangzhou Bay
Season	Four seasons	Four seasons	Summer	Summer	Four seasons
DIN ($\mu\text{mol}\cdot\text{dm}^{-3}$)	65–308	35–60	5.7–167.5	13.60–77.94	37.76–176.49
DIP ($\mu\text{mol}\cdot\text{dm}^{-3}$)	0.9–1.9	0.5–2	0.06–2.15	0.03–0.19	0.95–1.94
DSi ($\text{mg}\cdot\text{dm}^{-3}$)	35–146	140–220	1.8–147.2	4.8–91.3	30.59–108.89
TSM ($\text{mg}\cdot\text{dm}^{-3}$)	2–3519	100–140	1.5–229.4	6.6–3076	90–8390
Chl ($\text{mg}\cdot\text{m}^{-3}$)	0.3–15.3	2–15	0.1–32.5	1.05–14.49	0.84–2.97
Reference	[38,39]	[40]	[12,41]	[42]	This Study

4.2. Dynamics of PP and P^B

In temperate oceans, the saturated light intensities of phytoplankton usually vary from 33 to 400 $\mu\text{mol Einstein}\cdot\text{m}^{-2}\cdot\text{s}^{-1}$ [43]. As the dominant species of the HZB [18,19,44–47], diatoms’ saturated light intensities are usually above 50 $\mu\text{mol Einstein}\cdot\text{m}^{-2}\cdot\text{s}^{-1}$ [48]. This suggested that diatom light limitation would occur once LE lower than $2.2 \text{ Einstein}\cdot\text{m}^{-2}\cdot\text{day}^{-1}$. Our result showed the annual mean LE in the HZB was only $0.92 \text{ Einstein}\cdot\text{m}^{-2}\cdot\text{day}^{-1}$, much lower than saturated light level, indicating strong light limitation in the HZB. LE was higher than the saturated light intensity of phytoplankton only in the bay mouth of the HZB in summer. This was due to the significant increase of LE in the HZB caused by the northeastward movement of the Changjiang River secondary plume and the intrusion of low turbidity seawater. In this study, PP and P^B in the HZB showed significant negative

correlations with TSM only in summer ($r = -0.82$, $r = -0.93$, respectively) (Figure 7). This is mainly because the P^B of phytoplankton will increase with light when the phytoplankton was in the period of light limitation [48,49]. When the TSM decreases, PP and P^B will increase rapidly. Interestingly, there was no significant correlation between TSM and P^B in other seasons. This might be because TSM in these seasons is about five times higher than in summer, leading to LE being much lower than the saturated light intensity of phytoplankton. Thus, the variations of P^B and LE in the HZB in the same season lacked gradient, leading to weak correlations between them. In fact, LE and P^B had relatively consistent seasonal variations (i.e., summer > spring > winter (Figure A2)), indicating that TSM controlling LE was the main factor affecting phytoplankton photosynthesis.

Strong light limitation also led to excess nutrient in the HZB. Since light limitation cause that PP in the HZB was one order of magnitude lower than that of the CJE [4]. The phytoplankton in the HZB cannot uptake nutrients efficiently due to the light limitation. This causes terrigenous inputs of nutrients to accumulate in the HZB, leading to eutrophication. If the TSM concentration of the HZB decreases and the light limitation disappears, the HZB would turn into a potential high-PP region due to its abundant nutrient stocks.

4.3. Possible Effects of Zooplankton on Phytoplankton

In fact, the standing stock of phytoplankton is not only affected by light and nutrients but also related to the losses caused by respiration, zooplankton grazing, sinking and viral lysis [50,51]. Considering the re-suspension process caused by strong tidal mixing in the HZB, the loss of phytoplankton sinking might be negligible, so the losses of phytoplankton in the HZB are mainly controlled by zooplankton grazing.

In winter, although LE and P^B were relatively low, Chl were higher than those in spring and autumn in the HZB (Figure A2). This was probably because extremely high TSM in winter might affect the zooplankton grazing rate. Arruda et al. suggested that suspended particles can get into the zooplankton gut, potentially reducing food assimilation efficiency [52]. Herzig et al. suggested that sediment may also cause the abrasion of zooplankton exoskeletons during mixing [53]. On the other hand, the low temperature would prolong zooplankton development, reduce hatching abundance and decrease adult zooplankton survival [54]. This will lead to lower zooplankton biomass in winter, which reduces the grazing on phytoplankton. These factors might cause the low zooplankton grazing rate in highly turbid waters in winter, which made the accumulation of phytoplankton biomass in the water column. As a result, phytoplankton still had a relatively high Chl level in winter when P^B was low.

5. Conclusions

This study confirmed that LE levels of HZB were much lower than the requirement for phytoplankton growth, and light is the main limiting factor controlling Chl and PP levels in the area. Due to the low LE restricted by the extremely high TSM concentration, phytoplankton in most sea areas of the HZB is under the strong light limitation throughout the year. Nutrient concentrations did not affect the temporal and spatial distribution of phytoplankton. The nutrient-uptake rate of phytoplankton will decrease under the light limitation, resulting in the excess of nutrients, which is likely the important reason for the perennial eutrophication in the HZB. The inconsistent seasonal variation of Chl and P^B meant that the phytoplankton dynamics in the HZB were not only controlled by the bottom-up effect but also affected by the phytoplankton loss relevant to zooplankton. However, due to lacking of synchronous zooplankton grazing observations, it is difficult to assess seasonal variations in phytoplankton loss rates and their environmental control mechanisms. Further studies are required to understand the effects of phytoplankton dynamics in the HZB on the food web and eutrophication in the Zhoushan fishing ground. This requires not only longer-term interdisciplinary observations but also the studies of primary and secondary production coupling, especially the influence of highly turbid waters and strong tidal mixing on the phytoplankton loss rate.

Author Contributions: Conceptualization, Y.W. and Q.H.; methodology, Y.W. and Q.H.; validation, Q.H., J.C. and F.Z.; formal analysis, Q.H., J.C. and F.Z.; investigation, Q.H., J.C. and F.Z.; resources, Q.H., J.C. and F.Z.; data curation, Y.W.; writing—original draft preparation, Y.W.; writing—review and editing, Q.H., F.Z. and W.Z.; visualization, Y.W.; supervision, Q.H., J.C. and F.Z.; project administration, Q.H., J.C. and F.Z.; funding acquisition, Q.H., J.C. and F.Z. All authors have read and agreed to the published version of the manuscript. Y.W. and Q.H. contributed equally to this work and should be considered co-first authors.

Funding: The research was funded by National Natural Science Foundation of China-Zhejiang Informatization and Industrialization Integration Project (U1709201), National Natural Science Foundation of China (41876026), Zhejiang Provincial Ten Thousand Talents Plan (2020R52038); National Program on Global Change and Air-Sea Interaction (Phase II)—Hypoxia and Acidification Monitoring and Warning Project in the Changjiang Estuary, Scientific Research Fund of the Second Institute of Oceanography, MNR (SZ2001, JG1103), National Program of the Chinese Offshore Investigation and Assessment (908-ST04-I/II).

Institutional Review Board Statement: Not applicable.

Informed Consent Statement: Not applicable.

Data Availability Statement: Not applicable.

Acknowledgments: We thank NASA for providing satellite PAR product, and thank Chenggang Liu for collecting partly in-situ Chl data. We are grateful to both Dong Sun, Chenggang Liu and all reviewers for their valuable suggestions. We are also grateful to “Patrol 49” crews’ kindly help during the field investigations.

Conflicts of Interest: The authors declare no conflict of interest.

Appendix A

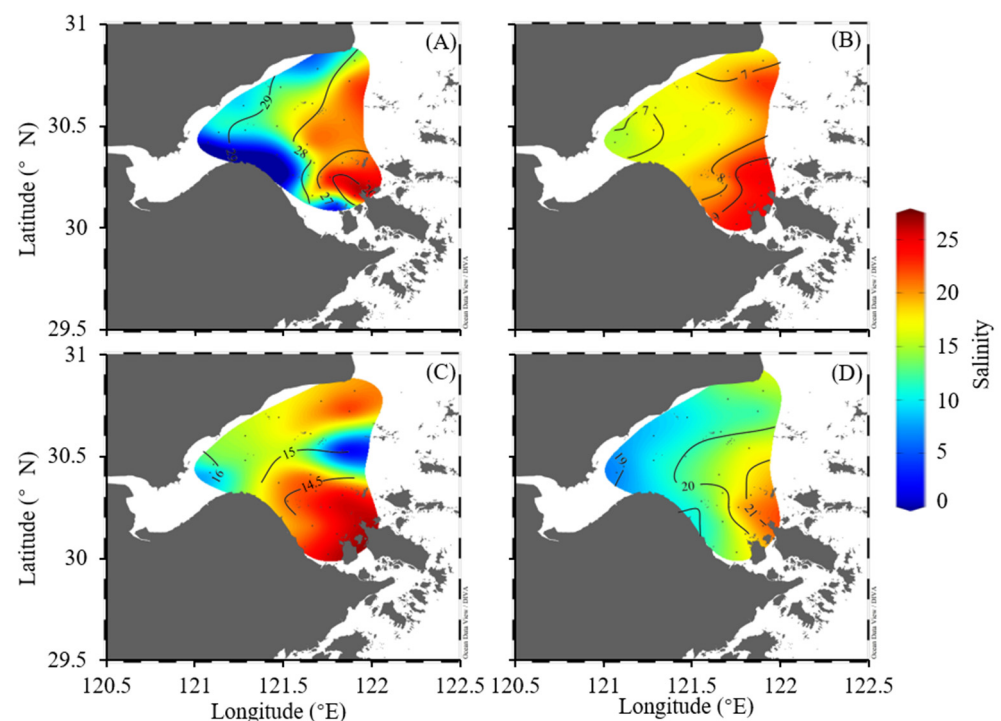


Figure A1. Spatial and temporal variations of surface salinity in (A) July 2006, (B) December 2006, (C) April 2007 and (D) October 2007. The black lines are the isolines of surface temperature (°C).

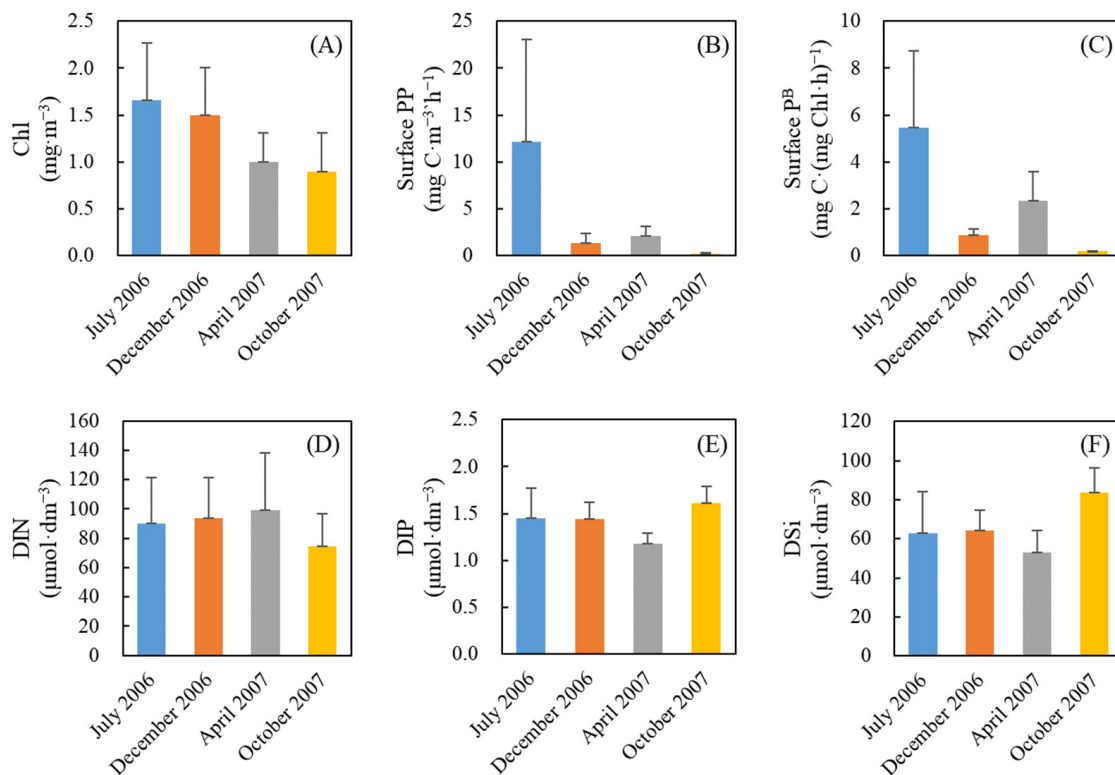


Figure A2. Seasonal variations of (A) the mean Chl in the mixed layer ($\text{mg}\cdot\text{m}^{-3}$), (B) surface PP ($\text{mg C}\cdot\text{m}^{-3}\cdot\text{h}^{-1}$), (C) surface P^B ($\text{mg C}\cdot(\text{mg Chl}\cdot\text{h})^{-1}$), (D) the mean DIN in the mixed layer ($\mu\text{mol}\cdot\text{dm}^{-3}$), (E) the mean DIP in the mixed layer ($\mu\text{mol}\cdot\text{dm}^{-3}$) and (F) the mean DSi in the mixed layer ($\mu\text{mol}\cdot\text{dm}^{-3}$).

References

- Tang, Q.; Su, J.; Sun, S.; Zhang, J.; Huang, D.; Jin, X.; Tong, L. A study of marine ecosystem dynamics in the coastal ocean of China. *Adv. Earth Sci.* **2005**, *20*, 1288–1299. [In Chinese with English Abstract].
- Zhou, F.; Chai, F.; Huang, D.; Xue, H.; Chen, J.; Xiu, P.; Xuan, J.; Li, J.; Zeng, D.; Ni, X.; et al. Investigation of hypoxia off the Changjiang Estuary using a coupled model of ROMS-CoSiNE. *Prog. Oceanogr.* **2017**, *159*, 237–254. [[CrossRef](#)]
- Hao, Q.; Chai, F.; Xiu, P.; Bai, Y.; Chen, J.; Liu, C.; Le, F.; Zhou, F. Spatial and temporal variation in chlorophyll *a* concentration in the Eastern China Seas based on a locally modified satellite dataset. *Estuar. Coast. Shelf Sci.* **2019**, *220*, 220–231. [[CrossRef](#)]
- Ning, X.; Shi, J.; Cai, Y.; Liu, C. Biological productivity front in the Changjiang Estuary and the Hangzhou Bay and its ecological effects. *Acta Oceanol. Sin.* **2004**, *26*, 96–106. [In Chinese with English Abstract].
- Zhou, F.; Chai, F.; Huang, D.; Wells, M.; Ma, X.; Meng, Q.; Xue, H.; Xuan, J.; Wang, P.; Ni, X.; et al. Coupling and decoupling of high biomass phytoplankton production and hypoxia in a highly dynamic coastal system: The Changjiang (Yangtze River) Estuary. *Front. Mar. Sci.* **2020**, *7*, 259. [[CrossRef](#)]
- Jin, X.; Shan, X.; Guo, X.; Li, X. Community structure of fishery biology in the Yangtze River estuary and its adjacent waters. *Acta Ecol. Sin.* **2009**, *29*, 4761–4772. [In Chinese with English Abstract].
- Xu, Y.; Yu, C.; Zhang, P.; Deng, X.; Zhang, Z.; Shen, H. Spring nekton community structure and its relationship with environmental variables in Hangzhou Bay-Zhoushan inshore waters. *J. Fish. China* **2019**, *43*, 605–617. [In Chinese with English Abstract].
- Xie, D.; Wang, Z.; Gao, S.; De Vriend, H.J. Modeling the tidal channel morphodynamics in a macro-tidal embayment, Hangzhou Bay, China. *Cont. Shelf Res.* **2009**, *29*, 1757–1767. [[CrossRef](#)]
- Gao, S.; Chen, J.; Jin, H.; Wang, K.; Lu, Y.; Li, H.; Chen, F. Characteristics of nutrients and eutrophication in the Hangzhou Bay and its adjacent waters. *J. Mar. Sci.* **2011**, *29*, 36–47. [In Chinese with English Abstract].
- Hu, Y.; Yu, Z.; Zhou, B.; Li, Y.; Yin, S.; He, X.; Peng, X.; Shum, C.K. Tidal-driven variation of suspended sediment in Hangzhou Bay based on GOCI data. *Int. J. Appl. Earth Obs. Geoinf.* **2019**, *82*, 101920. [[CrossRef](#)]
- Ning, X.; Liu, Z.; Cai, Y. A review on primary production studies for China seas in the past 20 years. *Donghai Mar. Sci.* **2000**, *18*, 13–20. [In Chinese with English Abstract].
- Li, W.; Ge, J.; Ding, P.; Ma, J.; Liu, D. Effects of dual fronts on the spatial pattern of chlorophyll-*a* concentrations in and off the Changjiang River Estuary. *Estuaries Coasts* **2021**, *44*, 1408–1418. [[CrossRef](#)]
- Zhou, H.; Sun, Z.; Li, B.; Wu, X.; Gong, M.; Yang, H. Distribution changes of suspended sediment concentration and its dynamic analysis in Xiangshan Bay, Zhejiang Province. *Mar. Sci. Bull.* **2014**, *33*, 694–702. [In Chinese with English Abstract].

14. Jia, H.; Shao, J.; Cao, L. Analysis of the changes and development trend of ecological environment in Hangzhou Bay. *Environ. Pollut. Control.* **2014**, *36*, 14–19, [In Chinese with English abstract].
15. Liu, Z.; Ning, X. Phytoplankton standing stock and primary production in the front of Hangzhou Bay. *Donghai Mar. Sci.* **1994**, *12*, 58–65, [in Chinese with English Abstract].
16. Liu, Z.; Ning, X.; Cai, Y. Primary productivity and standing stock of the phytoplankton in the Hangzhou Bay to the Zhoushan Fishing Ground during autumn. *Acta Oceanol. Sin.* **2001**, *23*, 93–99, [In Chinese with English Abstract].
17. Jiang, M.; Shen, X. Relationship between chlorophyll a and inorganic nitrogen and phosphate in the Changjiang estuary and its adjacent waters. *Mar. Fish.* **2004**, *26*, 35–39, [In Chinese with English Abstract].
18. Wei, N.; Hu, H.; Mao, H.; Huang, B.; Wang, J.; Wang, Y. Survey and study of phytoplankton ecology in Zhoushan fishing ground and adjacent waters. *Mar. Environ. Sci.* **2010**, *29*, 170–173, [In Chinese with English Abstract].
19. Jia, H.; Hu, H.; Shao, J.; Wang, Y.; Wei, N. Community structure and environmental factors of phytoplankton in Changjiang Estuary and adjacent sea in spring and autumn. *Mar. Environ. Sci.* **2013**, *32*, 851–855, [In Chinese with English Abstract].
20. Huang, B.; Wang, J.; Shen, M. Community structure of zooplankton in the offshore water of the northern Zhejiang. *Environ. Monit. China* **2012**, *28*, 64–68, [In Chinese with English Abstract].
21. Jia, H.; Tang, J.; Hu, H. The variation tendency of biodiversity and cause analysis in Hangzhou Bay from 1992 to 2012. *Acta Oceanol. Sin.* **2014**, *36*, 111–118, [In Chinese with English Abstract].
22. Su, J.; Wang, K. Changjiang river plume and suspended sediment transport in Hangzhou Bay. *Cont. Shelf Res.* **1989**, *9*, 93–111.
23. Su, J.; Wang, K.; Li, Y. Fronts and transport of suspended matter in the Hangzhou Bay. *Acta Oceanol. Sin.* **1992**, *12*, 1–15.
24. National Aeronautics and Space Administration OceanColor. Available online: <https://oceancolor.gsfc.nasa.gov> (accessed on 2 April 2021).
25. Castillo Ramirez, A.; Santamaria Angel, E.; Gonzalez Silvera, A.; Frouin, R.; Sebastia Frasquet, M.T.; Tan, J.; Lopez Calderon, J.; Sanchez Velasco, L.; Enriquez Paredes, L. A new algorithm to estimate diffuse attenuation coefficient from Secchi disk depth. *J. Mar. Sci. Eng.* **2020**, *8*, 558. [[CrossRef](#)]
26. Knap, A.; Michaels, A.; Close, A.; Ducklow, H.; Dickson, A. *Protocols for the Joint Global Ocean Flux Study (JGOFS) Core Measurements*; JGOFS Rep. No19 Repr. IOC Man. Guides No. 29; UNESCO-IOC: Paris, France, 1994; Volume 19, p. 170.
27. Nielsen, S. The use of radioactive carbon (C^{14}) for measuring organic production in the sea. *J. Du Cons.* **1952**, *18*, 117–140. [[CrossRef](#)]
28. Ning, X.; Vaulot, D.; Liu, Z. Standing stock and production of phytoplankton in the estuary of the Chang-jiang (Yangtse River) and the adjacent East China Sea. *Mar. Ecol. Prog. Ser.* **1988**, *49*, 141–150. [[CrossRef](#)]
29. Evans, C.; O'Reilly, J.E.; Thomas, J. *A Handbook for the Measurement of Chlorophyll and Primary Production*; Texas A&M University: College Station, TX, USA, 1987; pp. 1–114.
30. Parsons, T.R.; Maita, Y.; Lalli, C. *A Manual of Chemical and Biological Methods for Seawater Analysis*; Pergamon Press: Oxford, UK, 1984; pp. 101–173.
31. Schlitzer, Reiner, Ocean Data View. Available online: <https://odv.awi.de> (accessed on 20 January 2022).
32. Justić, D.; Rabalais, N.N.; Turner, R.E.; Dortch, Q. Changes in nutrient structure of river-dominated coastal waters: Stoichiometric nutrient balance and its consequences. *Estuar. Coast. Shelf Sci.* **1995**, *40*, 339–356. [[CrossRef](#)]
33. Redfield, A.C.; Ketchum, B.H.; Richards, F.A. The influence of organisms on the composition of sea-water. *Sea* **1963**, *2*, 26–77.
34. Dortch, Q.; Whittedge, T.E. Does nitrogen or silicon limit phytoplankton production in the Mississippi River plume and nearby regions? *Cont. Shelf Res.* **1992**, *12*, 1293–1309. [[CrossRef](#)]
35. Wang, K.; Chen, J.; Jin, H. Nutrient structure and limitation in Changjiang River Estuary and adjacent East China Sea. *Acta Oceanol. Sin.* **2013**, *35*, 128–136, [In Chinese with English Abstract].
36. Liu, X.; Xiao, W.; Landry, M.R.; Chiang, K.-P.; Wang, L.; Huang, B. Responses of phytoplankton communities to environmental variability in the East China Sea. *Ecosystems.* **2016**, *19*, 832–849. [[CrossRef](#)]
37. Xu, Z.; Chen, Y.; Meng, X.; Wang, F.; Zheng, Z. Phytoplankton community diversity is influenced by environmental factors in the coastal East China Sea. *Eur. J. Phycol.* **2016**, *51*, 107–118. [[CrossRef](#)]
38. Guesdon, S.; Stachowski-Haberkorn, S.; Lambert, C.; Beker, B.; Brach-Papa, C.; Auger, D.; Bechemin, C. Effect of local hydroclimate on phytoplankton groups in the Charente estuary. *Estuar. Coast. Shelf Sci.* **2016**, *181*, 325–337. [[CrossRef](#)]
39. Modéran, J.; David, V.; Bouvais, P.; Richard, P.; Fichet, D.J.E.; Coastal. Organic matter exploitation in a highly turbid environment: Planktonic food web in the Charente estuary, France. *Estuar. Coast. Shelf Sci.* **2012**, *98*, 126–137. [[CrossRef](#)]
40. Nagy, G.J.; Gomez-Erache, M.; Lopez, C.H.; Perdomo, A.C. Distribution patterns of nutrients and symptoms of eutrophication in the Rio de la Plata River Estuary System. *Hydrobiologia* **2002**, *475*, 125–139. [[CrossRef](#)]
41. Zhou, W.; Yuan, X.; Huo, W.; Yin, K. Distribution of chlorophyll a and primary productivity in the adjacent sea area of Changjiang River Estuary. *Acta Oceanol. Sin.* **2004**, *26*, 143–150, [In Chinese with English Abstract].
42. Wang, Y.; Liu, D.; Lee, K.; Dong, Z.; Di, B.; Wang, Y.; Zhang, J. Impact of Water-Sediment Regulation Scheme on seasonal and spatial variations of biogeochemical factors in the Yellow River Estuary. *Estuar. Coast. Shelf Sci.* **2017**, *198*, 92–105. [[CrossRef](#)]
43. Singh, S.P.; Singh, P. Effect of temperature and light on the growth of algae species: A review. *Renew. Sustain. Energy Rev.* **2015**, *50*, 431–444. [[CrossRef](#)]
44. Zhang, Y.; Yu, J.; Jiang, Z.; Wang, Q.; Wang, H. Variations of summer phytoplankton community related to environmental factors in a macro-tidal estuarine embayment, Hangzhou Bay, China. *J. Ocean. Univ. China* **2015**, *14*, 1025–1033. [[CrossRef](#)]

45. Qin, M.; Cai, Y.; Wang, X.; Wei, Y.; Ren, M.; Ge, C. Analysis and assessment on eutrophication in Hangzhou Bay. *Mar. Environ. Sci.* **2009**, *28*, 53–56, [In Chinese with English Abstract].
46. Li, L.; Zang, J.; Liu, J.; Liu, W.; Yin, X.; Zhang, B.; Ran, X. Phosphate Distribution, Variation and Its Relationship with Phytoplankton Changes in the Qiantangjiang River Estuary. *Adv. Mar. Sci.* **2018**, *36*, 279–289, [In Chinese with English Abstract].
47. Zhou, Y.; Zhao, C.; Gao, Y.; Long, H.; Yu, J. Variation and distribution characteristics of phytoplankton in ecology-monitoring area of Hangzhouwan Bay from 2005 to 2008. *J. Mar. Sci.* **2010**, *28*, 28–35, [In Chinese with English Abstract].
48. Sarthou, G.; Timmermans, K.R.; Blain, S.; Tréguer, P. Growth physiology and fate of diatoms in the ocean: A review. *J. Sea Res.* **2004**, *53*, 25–42. [[CrossRef](#)]
49. Cloern, J.E.; Dufford, R. Phytoplankton community ecology: Principles applied in San Francisco Bay. *Mar. Ecol. Prog. Ser.* **2005**, *285*, 11–28. [[CrossRef](#)]
50. Behrenfeld, M.J.; Boss, E.S. Resurrecting the ecological underpinnings of ocean plankton blooms. *Ann. Rev. Mar. Sci.* **2014**, *6*, 167–208. [[CrossRef](#)] [[PubMed](#)]
51. Hoover, R.S.; Hoover, D.; Miller, M.; Landry, M.R.; DeCarlo, E.H.; Mackenzie, F.T. Zooplankton response to storm runoff in a tropical estuary: Bottom-up and top-down controls. *Mar. Ecol. Prog. Ser.* **2006**, *318*, 187–201. [[CrossRef](#)]
52. Arruda, J.A.; Marzolf, G.R.; Faulk, R.T. The role of suspended sediments in the nutrition of zooplankton in turbid reservoirs. *Ecology* **1983**, *64*, 1225–1235. [[CrossRef](#)]
53. Herzig, A. The zooplankton of the open lake. In *Neusiedlersee: The Limnology of a Shallow Lake in Central Europe*; Löffler, H., Ed.; Springer: Dordrecht, The Netherlands, 1979; pp. 281–335.
54. Gillooly, J.F.; Charnov, E.L.; West, G.B.; Savage, V.M.; Brown, J.H. Effects of size and temperature on developmental time. *Nature* **2002**, *417*, 70–73. [[CrossRef](#)]